



Society of Petroleum Engineers

SPE-230115-MS

Benchmarking DAS Interrogator Performance for Flow Monitoring Applications: A Broadband Study with Mechanical, Acoustic, and Turbulent Flow Stimuli

P. Moradi, N. Kalia, and J. Noguera, Baker Hughes, Houston, TX, USA

Copyright 2025, Society of Petroleum Engineers DOI [10.2118/230115-MS](https://doi.org/10.2118/230115-MS)

This paper was prepared for presentation at the ADIPEC held in Abu Dhabi, UAE, 3 – 6 November 2025.

This paper was selected for presentation by an SPE program committee following review of information contained in an abstract submitted by the author(s). Contents of the paper have not been reviewed by the Society of Petroleum Engineers and are subject to correction by the author(s). The material does not necessarily reflect any position of the Society of Petroleum Engineers, its officers, or members. Electronic reproduction, distribution, or storage of any part of this paper without the written consent of the Society of Petroleum Engineers is prohibited. Permission to reproduce in print is restricted to an abstract of not more than 300 words; illustrations may not be copied. The abstract must contain conspicuous acknowledgment of SPE copyright.

Abstract

This paper presents a systematic workflow to evaluate the performance of Distributed Acoustic Sensing (DAS) interrogators for flow monitoring applications under controlled laboratory conditions. Broadband responses are assessed using benchtop testbeds equipped with standard and engineered fiber-optic sensors, each subjected to meter- and sub-meter-scale stimuli that emulate downhole flow phenomena. The methodology incorporates four primary stimuli: mechanical waveform injection via calibrated piezoelectric actuators across a wide frequency and amplitude range; acoustic waveform injection using multiple modulation schemes to simulate non-contact sensing; flow-induced waveforms from turbulent gas flow to measure phase response and coherence; and thermal stimulation. To assess signal fidelity under realistic conditions, the setup integrates polarization controllers and axial translation modules that simulate disturbances typical of mobile conveyance systems such as wireline and coiled tubing. The results reveal that conventional testing protocols can be effectively complemented by additional benchtop tests utilizing diverse stimuli, supporting broadband performance validations essential for accurate flow monitoring applications. This comprehensive evaluation de-risks technology selection and helps unlock the full potential of DAS for complex in-well flow characterization.

Introduction

Distributed Acoustic Sensing (DAS) has emerged as a transformative technology in the energy sector, converting entire lengths of fiber-optic cable into a dense array of thousands of acoustic sensors. Initially proven in applications such as Vertical Seismic Profiling (VSP), microseismic monitoring, and well integrity surveillance, DAS provides unprecedented spatial and temporal resolution for observing downhole dynamics (Daley *et al.* 2013, Lindsey *et al.* 2020, Hull *et al.* 2017, Verdon *et al.* 2020). However, the industry is increasingly pushing the boundaries of this technology toward more demanding applications, particularly the quantitative characterization of single- and multi-phase fluid flow within the wellbore (Ünalmsis 2022, Xiao *et al.* 2015, Farhadiroushan *et al.* 2021, Moradi *et al.* 2024). Applications like production allocation, injection profiling, and leak detection demand a level of sensitivity and fidelity that challenges the conventional understanding and deployment of DAS systems.

The success of a downhole DAS monitoring project depends on the meticulous integration and optimization of every element in a complex, interdependent system (Figure 1):

- **Interrogation Unit:** The interrogator is the core of the system, employing optical reflectometry to measure localized strain or strain rate. The primary technique is Phase-sensitive Optical Time-Domain Reflectometry (Φ -OTDR), which detects minute phase shifts in Rayleigh backscattered light induced by external acoustic energy. An alternative approach, Optical Frequency-Domain Reflectometry (OFDR), provides superior spatial resolution over shorter sensing ranges. The interrogator's performance is governed by parameters such as laser characteristics, sampling rate, and gauge length (i.e., the spatial averaging window). These factors collectively define key performance metrics—including frequency response, spatial resolution, and signal-to-noise ratio (SNR).
- **Data Acquisition and Processing Workflows:** DAS systems generate enormous volumes of data—often several terabytes per day during a typical survey—which poses a substantial operational challenge. Without streamlined, efficient, and well-established workflows for data handling, processing, and interpretation, this vast dataset can easily lead to delays, frustration, or inconclusive outcomes. As such, the success of DAS applications hinges not only on the hardware, but equally on the robustness of the signal processing algorithms and the effectiveness of the data management strategy.
- **Sensing Element:** This component comprises the single-mode fiber (e.g., standard or enhanced backscatter fiber (EBF)) and its mechanical coupling to the conveying string or production tubing.

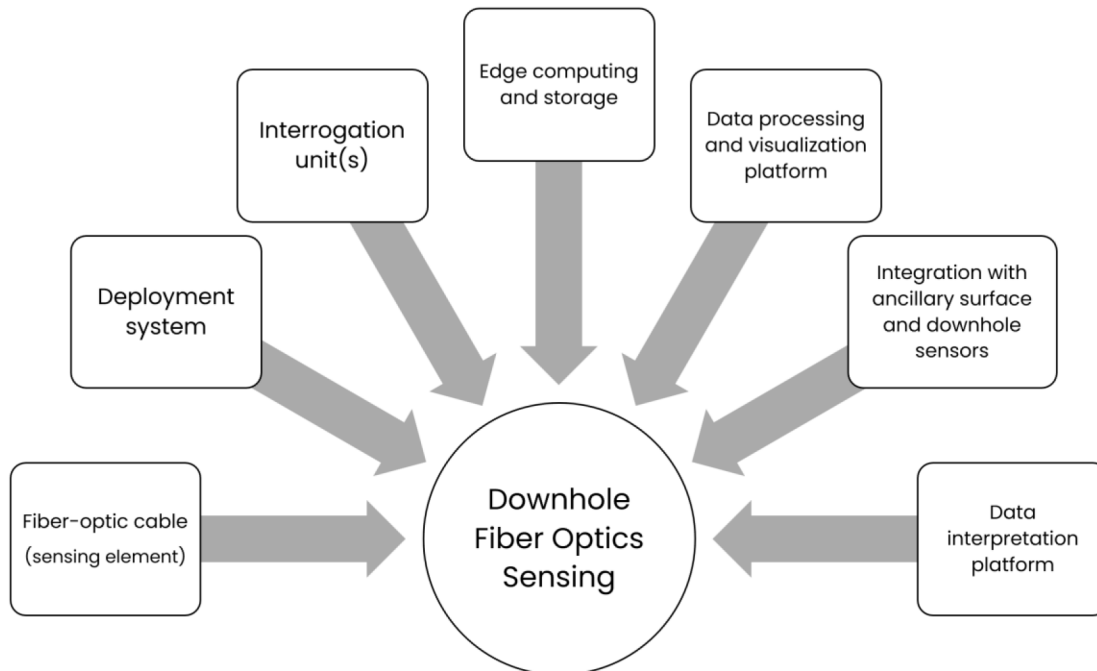


Figure 1—System of components in a downhole fiber-optic sensing project, illustrating the critical components from the in-well fiber sensor to the data analytics platform. The successful integration of each element is vital for transforming raw optical measurements into actionable intelligence.

The focus of this work is on the performance evaluation of DAS interrogators. Given DAS's growing promise for flow monitoring, introducing standardized performance benchmarks tailored to this specific application presents a clear opportunity. Conventional testing methodologies—often centered on self-noise characterization or mechanical waveform injection for seismic-scale applications—may be insufficient for assessing a system's ability to detect the subtle, broadband, and small-scale signatures

associated with fluid flow, which demand high-fidelity, broadband measurement. To address this gap, the paper presents a systematic methodology for benchmarking DAS interrogator performance under controlled laboratory conditions. By subjecting both standard and engineered fibers to a suite of calibrated mechanical, acoustic, thermal, and turbulent flow stimuli, the study moves beyond traditional metrics. The workflow enables quantitative assessment of critical performance attributes, including broadband frequency and phase response, sensitivity to meter- and sub-meter-scale events, and stability under dynamic conditions—ultimately helping operators and service providers mitigate operational risks, select appropriate technologies, and unlock the full quantitative potential of DAS for in-well fluid flow characterization.

The following sections introduce each test and present sample results, progressing from fundamental benchmarks to advanced, application-specific evaluations. A key aspect of the workflow is the evaluation of interrogator performance across varying gauge lengths. To achieve this, each test is repeated three times, with the DAS interrogator configured and optimized for one of three distinct gauge lengths: sub-meter, 1–2 meters, and 10 meters. Optimization involves adjusting the interrogator’s optical pulse width and internal acquisition parameters for each configuration. This approach yields three distinct datasets per stimulus, ensuring the system is assessed under its optimal operating conditions and enabling a direct, representative evaluation of the hardware’s capabilities.

Self-noise and loss budget

To evaluate the intrinsic noise floor of the interrogators, self-noise tests are conducted under quiet conditions with no external stimulus. This self-noise is the fundamental noise level of the phase or strain measured by the interrogator and is one of the most important performance parameters, as it defines the minimum detectable signal and ultimately governs the system's sensitivity. Concurrently, the optical loss budget evaluation determines the maximum optical attenuation the system can tolerate before the signal-to-noise ratio degrades unacceptably, thereby defining its maximum operational range and deployment constraints.

Experimental Apparatus

The test utilizes a 5 km fiber spool that is acoustically isolated to prevent environmental vibrations from influencing the measurement. Data is collected from three distinct fiber sections located at distances of 500, 2000, and 4500 m along the fiber. For each section, 300 consecutive sensing channels are analyzed. Time-series data, collected over 180 seconds, is converted to amplitude spectral density (ASD) plots using a Fast Fourier Transform (FFT) with a Blackman-Harris window. The results are normalized to a 1 Hz bandwidth and expressed in units of strain per root-Hertz (strain/ $\sqrt{\text{Hz}}$). These plots reveal the baseline noise characteristics of the interrogator across its frequency range and provide insight into its sensitivity limits. To assess the interrogator's robustness to signal loss, the self-noise measurements are repeated after inserting 3 dB and 5 dB optical attenuators into the fiber path near the interrogator. This test can also be performed using a variable optical attenuator, where measurements are made while the attenuation is incrementally increased. By plotting the noise floor as a function of the added two-way optical loss (in dB), we can identify the point at which the noise floor begins to rise sharply. This inflection point defines the practical loss budget of the interrogator, providing a critical specification for designing and deploying DAS systems over long distances or through networks with multiple connectors and splices.

Sample Results

[Figure 2](#) compares the self-noise performance at a 10 m gauge length for two sample interrogators, both tested using standard single-mode fiber. The results highlight a marked difference in the intrinsic noise levels of the two interrogator systems, even under identical fiber and test conditions. Additionally, the change in noise floor with increasing distance from the interrogator appears to differ between the two sample datasets. [Figure 3](#) explores the impact of fiber type on system noise by comparing the self-noise measured when using a standard fiber against the results from two different types of EBF. The results show a substantial

improvement in the noise floor when using EBF, which is promising as this fiber offers superior performance for flow monitoring applications due to its higher level of Rayleigh backscatter. Notably, EBF Type A exhibits the lowest noise floor, underscoring performance variation among enhanced fiber designs.

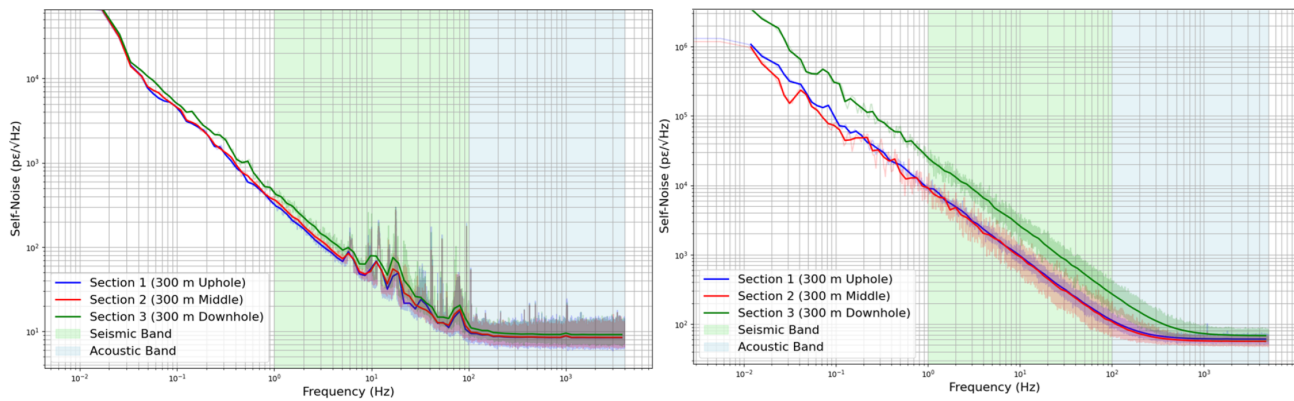


Figure 2—Self-noise comparison for two interrogators optimized at a 10-meter gauge length. The measurements, conducted along 300-meter sections over 180-second periods, reveal a noticeable difference in self-noise between the two interrogators.

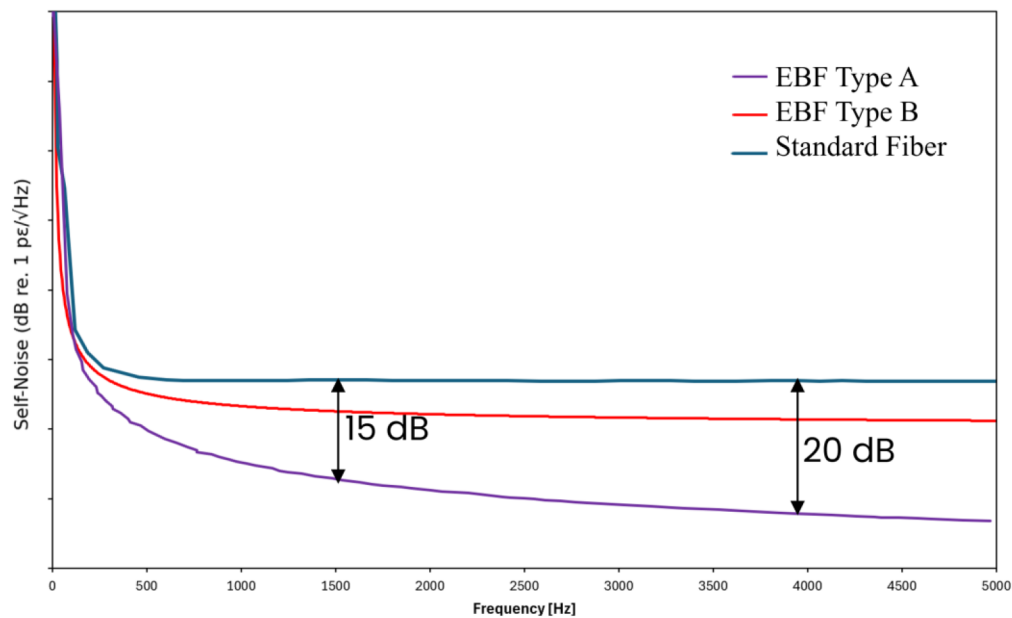


Figure 3—Comparison of an interrogator's self-noise measured using standard fiber versus two different EBF types. The plots show a substantial improvement in the measured noise floor when using EBF compared to standard fiber. EBF Type A demonstrates the lowest noise floor, highlighting the performance variation among different enhanced fiber designs.

Figure 4 compares the strain-rate self-noise performance of four sample interrogators using EBF Type A as the sensing fiber. The results show noticeable variation in performance, a difference that directly impacts the accuracy of broadband strain-rate-dependent measurements such as SoS and the characterization of transient acoustic events. Even when using the same fiber type and gauge length, interrogator-specific design choices have influenced the system's ability to preserve high-frequency content and maintain low noise floors.

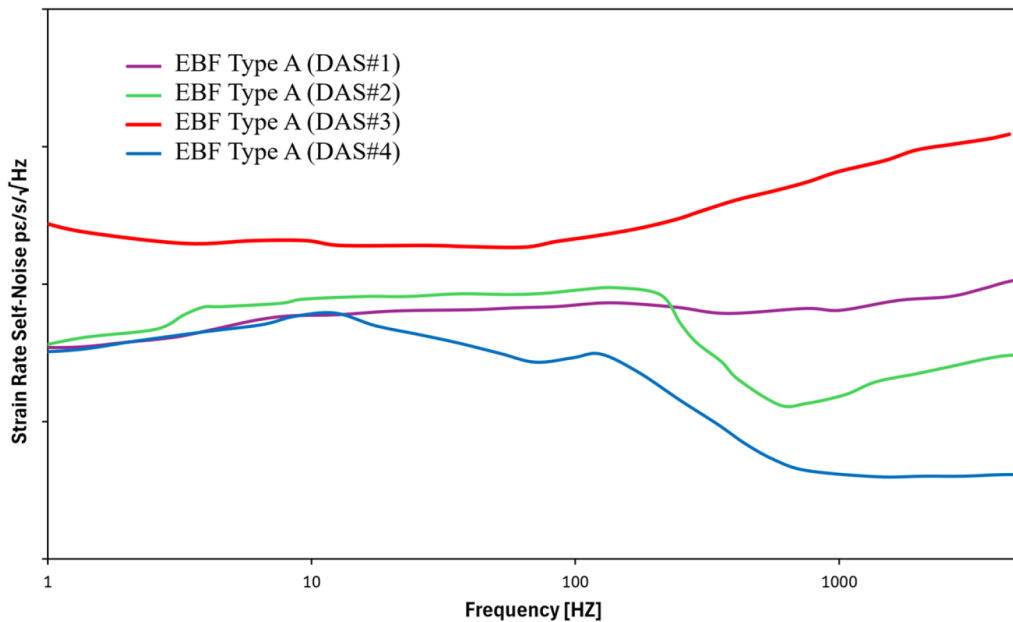


Figure 4—Comparison of strain-rate self-noise for four different interrogators using EBF Type A sensing fiber. The results show a significant variation in performance, highlighting that the choice of interrogator is a critical factor for the accuracy of strain-rate-sensitive measurements such as SoS.

The sample self-noise results underscore the importance of interrogator and fiber selection as a strategic choice that must be aligned with the sensing objectives and expected signal characteristics of the deployment environment.

Turbulent Flow Stimulus

While single-frequency mechanical actuators are essential for determining a DAS system's transfer function, downhole fluid flow generates a broadband acoustic signature that is fundamentally different. The primary source of this signature is turbulent pressure fluctuations within the fluid. Therefore, to properly evaluate an interrogator's performance for flow monitoring, it is crucial to test its response to a stimulus that mimics this turbulent environment. The turbulent flow test bed is designed to measure the DAS system's sensitivity to broadband noise generated by controlled gas flow, extending beyond the scope of current standards. Here, we explicitly aim to measure the phase coherence of the DAS signal, a critical metric that quantifies the stability and consistency of the signal's phase relationship between different points in space and time. High phase coherence is a prerequisite for advanced flow analysis techniques, such as determining the SoS from the acoustic field.

Experimental Apparatus

A dedicated 2.5-meter-long test rig is constructed to generate controlled turbulent flow across a section of fiber, as shown in Figure 5. The apparatus features a flow annulus created by a 2-inch outer diameter stainless steel inner pipe placed concentrically within a 4.5-inch inner diameter PVC outer pipe. A 45-meter segment of EBF Type A is helically wrapped with a consistent pitch around the outer surface of the inner steel pipe. This configuration ensures that a sufficient length of fiber, spanning multiple DAS gauge lengths, is exposed to flow-induced vibrations within the compact test section. The helical geometry is critical for exposing the fiber to a wide range of wavelengths, an objective nearly impossible to achieve with a straight fiber segment in a benchtop setup.

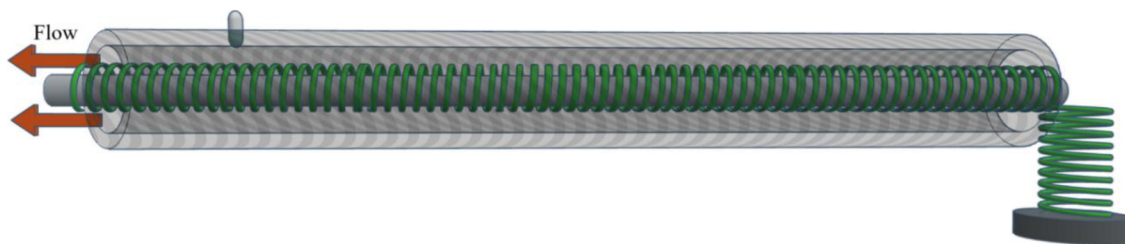


Figure 5—Schematic of the turbulent flow stimulus apparatus. The setup consists of concentric pipes that create an annulus for controlled air flow, which is measured by anemometers. A 45-meter segment of EBF Type A is helically wrapped around the 2.5-meter-long inner steel pipe to serve as the sensing element. This apparatus allows for measuring the response to broadband turbulent flow noise to quantitatively assess the DAS system's phase coherence and sensitivity to flow-induced vibrations.

It is important to note that this setup is designed to measure the fiber's response to sound waves induced by the turbulent boundary layer, which is distinct from applications that measure the bulk hoop strain of the pipe itself. Upstream of the flow section, a 500-meter fiber spool is included to constantly monitor the system's intrinsic noise floor, providing a stable reference against which flow-induced signals are measured. To ensure the measurement captures the direct response to the flow field rather than resonant artifacts, the downstream end of the flow loop is designed with a perforated outlet to minimize backpressure and prevent the formation of acoustic standing waves. The velocity of the pressurized air flowing through the annulus is measured and monitored using a set of calibrated anemometers, providing an independent, quantitative measure of the input stimulus.

Sample Results

The experiments are conducted under three distinct flow scenarios to characterize the system's response across different energy levels and stimulation methods. The first scenario establishes a low-velocity regime where the annular air velocity is maintained below 0.4 m/s, serving to characterize the system's sensitivity to incipient flow. In the second scenario, the flow velocity is doubled to approximately 0.8 m/s. This condition introduces significantly higher turbulent energy, allowing for the evaluation of the system's dynamic range and its response to a more energetic, broadband acoustic field. The final scenario involves stimulating the flow using a proprietary methodology designed to boost the coherence and amplitude of the flow-induced acoustic signature, enabling a more robust characterization of the system's phase response and its ultimate detection limits. By analyzing the data from these scenarios, particularly in the frequency-wavenumber domain, we can determine the frequency and wavenumber range over which the DAS system maintains a coherent phase response, providing a direct and quantitative benchmark of its capability for advanced flow characterization.

The efficacy of the turbulent flow stimulus test in differentiating interrogator performance is demonstrated in Figure 6. Figure 6–left depicts a sample result from a high-performance DAS interrogator responding to the turbulent flow. The data, transformed into the f-k domain, exhibits distinct and coherent linear features that represent sound waves propagating through the fluid medium. The slope of these linear features directly corresponds to the SoS. The high SNR and strong phase coherence of this measurement enable the application of advanced processing techniques. For instance, using the GPU-accelerated Phase-weighted Convolution (GPC) method (Moradi 2025), the upgoing and downgoing SoS can be measured, enabling accurate determination of flow velocity from acoustic data, showcasing the system's ability to provide quantitative insights (Figure 7). In contrast, Figure 6–right illustrates results from a system that underperforms in adequately capturing the acoustic field under the exact same stimulus conditions. The corresponding f-k plot lacks discernible coherent energy corresponding to the propagating sound waves. The signal is diffuse, and the phase information is unstable, making it challenging to resolve the acoustic

wavefronts. Consequently, for this dataset quantitative analysis such as SoS determination is not feasible, as the system is not optimized for collecting data with sufficient fidelity.

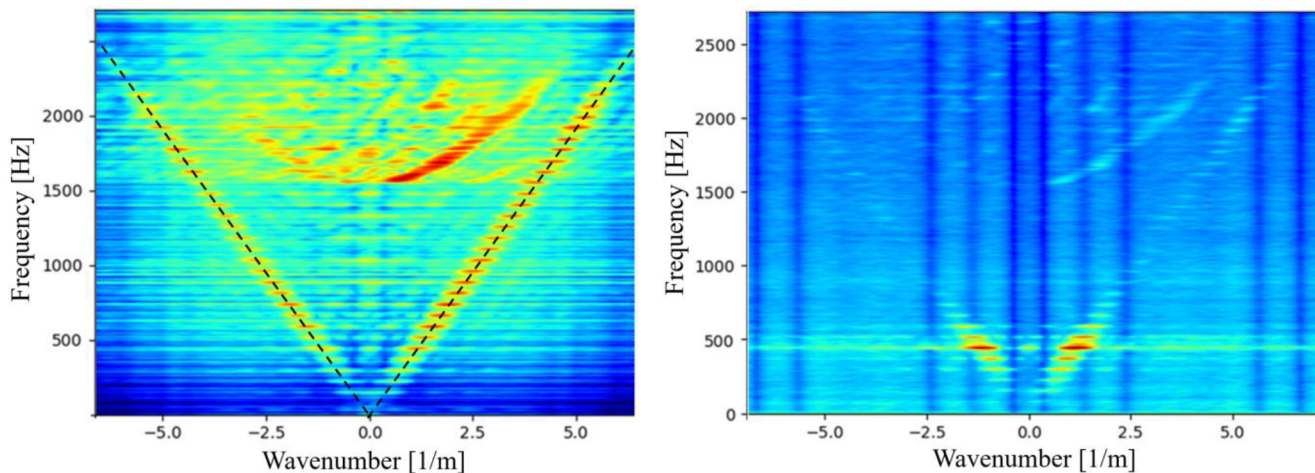


Figure 6—Comparison of interrogator performance using f-k analysis of turbulent flow data. (A) An f-k plot from a sample high-performance interrogator shows clear, coherent linear features corresponding to propagating sound waves. The slope of these features directly yields the SoS. (B) An f-k plot from a lower-performance system under identical flow conditions. The same color scale range is used for both plots.

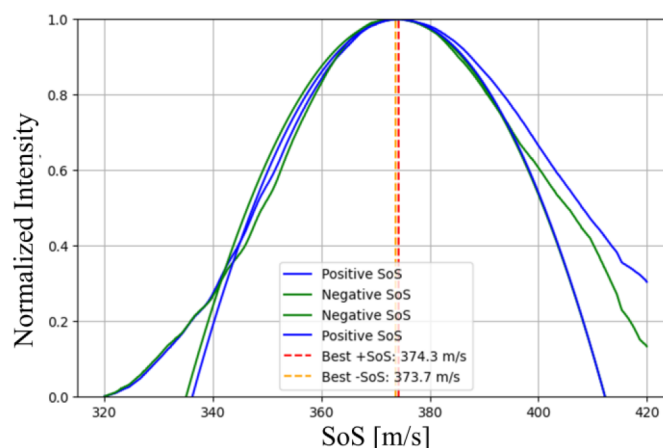


Figure 7—Measuring SoS using the GPC method. Applying the method to space-time acoustic data results in intensity plots where the peak corresponds to the velocity at which the signal phase is most coherent across the sensor array. This peak value provides a robust, quantitative measurement of the SoS in the fluid, both upstream and downstream of the flow direction.

This direct comparison highlights the critical importance of evaluating DAS systems with realistic, broadband stimuli to certify their fitness-for-purpose in demanding flow monitoring applications. Notably, the system exhibiting limited coherence in this test configuration demonstrated a lower self-noise floor than the high-performance system. This finding reinforces that a low self-noise level is not a sufficient indicator of a system's ability to resolve coherent signals under dynamic stimulus conditions.

Acoustic Waveform Injection

In many downhole flow monitoring applications, the fiber-optic cable does not have direct mechanical contact with the flowing fluid(s) inside the well. For example, when conveyed inside Coiled Tubing (CT) or permanently installed behind production casing, the fiber is mechanically decoupled from the reservoir flow. Instead, acoustic pressure waves—generated by flow phenomena such as eddies, restrictions, valve operations, or multiphase slugging—propagate through the completion hardware (e.g., steel tubing,

cement sheath) and induce micro-strains on the fiber. Accurate detection of these indirect acoustic signals is therefore critical. This test section departs from conventional DAS testing, which typically relies on direct mechanical excitation, and instead evaluates interrogator performance in response to structure-borne acoustic waves. The goal is to characterize the system's sensitivity and fidelity under a range of controlled acoustic stimuli. This methodology enables a nuanced assessment of the interrogator's ability to capture complex, broadband, and non-stationary signals—key for quantitative interpretation in indirect sensing environments.

Experimental Apparatus

To conduct these tests, a controlled acoustic environment is created using a sealed, insulated enclosure, as depicted in Figure 8. Inside the enclosure, calibrated loudspeakers are positioned to project sound waves uniformly toward 2000 m test coils of both standard fiber and EBF Type A. This setup ensures that any measured signal is a direct result of the acoustic stimulus, isolated from ambient laboratory noise. There are also two optical attenuators at known locations upstream of the main test coils. These attenuators create sections with a slightly reduced optical power level.

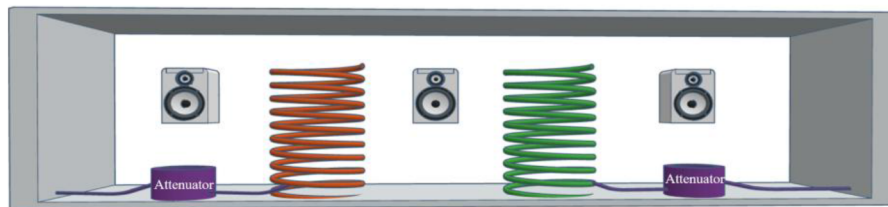


Figure 8—Schematic of the acoustic waveform injection test setup. Loudspeakers project controlled acoustic signals (FSK, PSK, chirp, and broadband audio) toward coils of both standard fiber and EBF within a sealed, insulated enclosure. The setup includes optical attenuators at known locations to simulate signal degradation.

Four distinct acoustic waveforms are designed, each with a known spectral content, to probe different aspects of the DAS interrogator's performance. First, a broadband audio signal, specifically a music file with a complex and dynamic spectral content, is used. This stimulus serves a purpose similar to the turbulent flow test, evaluating the system's ability to faithfully reproduce a complex, non-stationary waveform across a wide frequency range and assessing its overall dynamic fidelity. Second, a Multiple Frequency-Shift Keying (MFSK) modulated signal is employed. This waveform consists of a carrier that shifts between multiple discrete, known frequency states, each corresponding to a unique symbol in a coded sequence. By using more than two frequencies, this test efficiently probes the interrogator's response across a wider set of specific tones within a single measurement. It is designed to quantitatively assess the system's frequency accuracy and its ability to rapidly and precisely resolve distinct tonal changes. Third, a Phase-Shift Keying (PSK) signal is used to directly challenge the phase fidelity of the DAS measurement. In a PSK signal, information is encoded not in the amplitude or frequency, but in the phase of a constant-frequency carrier wave. Finally, a linear frequency-modulated chirp signal is utilized. This waveform sweeps continuously from a low to a high frequency over a set duration. It provides an efficient method for mapping the system's complete frequency response function, identifying any potential frequency-dependent variations in sensitivity, resonances within the test apparatus, or limitations in the interrogator's effective bandwidth.

Sample Results

The results from the acoustic waveform injection tests provide a method for assessing interrogator fidelity. Figure 9 compares the performance of three sample DAS interrogators when exposed to a linear chirp stimulus. The top row shows the spectrogram recorded by the first system, which closely tracks the frequency sweeps across the tested bandwidth. This is evidenced by sharp, continuous lines with high signal-to-noise ratio, yielding a 92% similarity to the reference waveform. The middle row presents the

response from the second interrogator under identical conditions. Here, the spectrogram reveals noticeable degradation, with 45% similarity to the injected signal—indicating reduced capability in capturing non-stationary frequency content. The bottom row illustrates the output from the third interrogator, which suffers from aliasing artifacts due to an insufficient sampling rate. The chirp structure is obscured by overlapping spectral components. Qualitative auditory analysis, performed by converting the recorded time-series data back into an audio file, confirms these quantitative findings; the first interrogator produces a clear and recognizable reproduction of the original sound played inside the test box, while the second and third yield distorted and muffled versions.

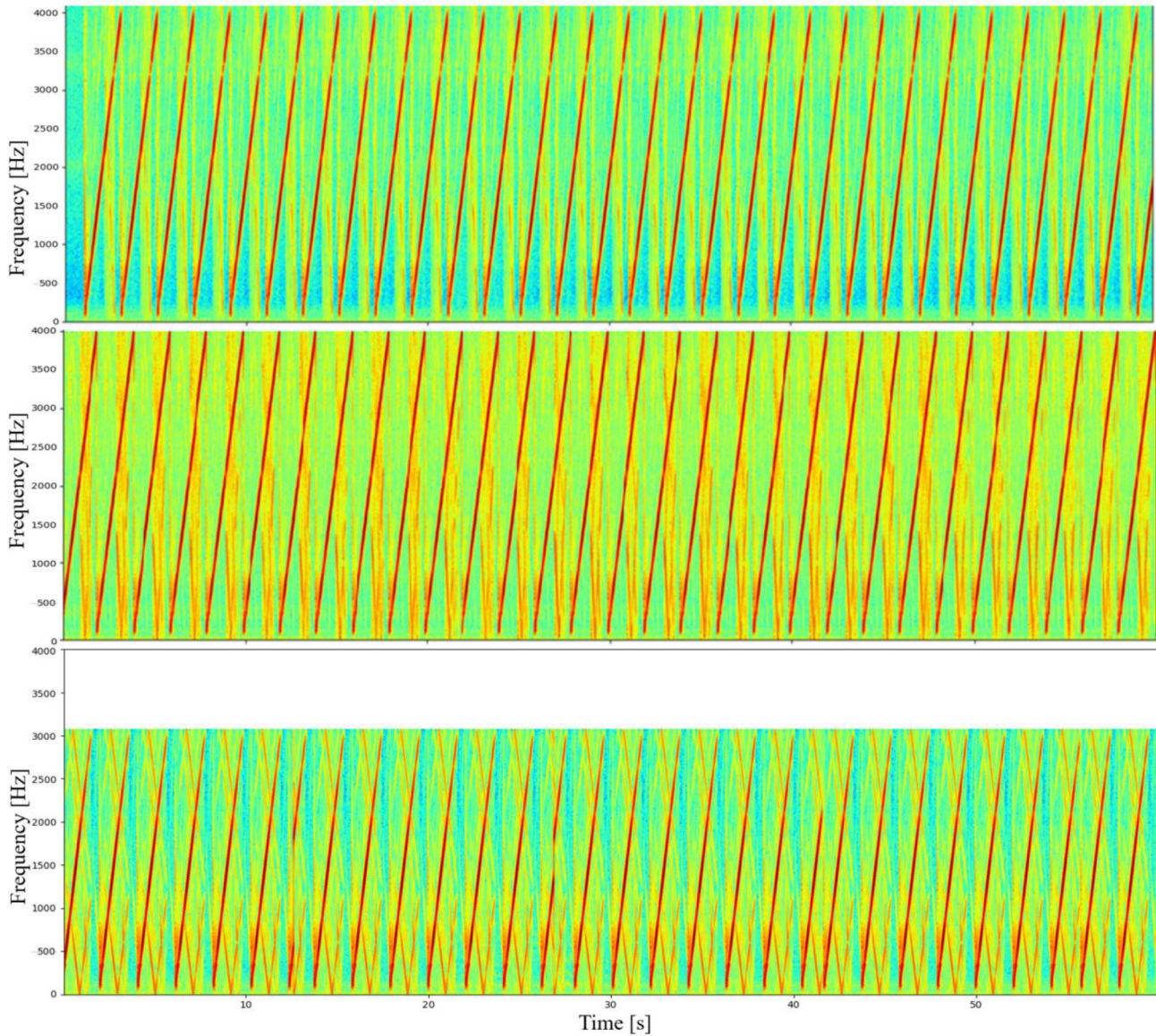


Figure 9—Comparison of interrogator performance in response to linear chirp acoustic stimulus. The top row shows the spectrogram recorded by a system with high fidelity to the original injected chirp signal. The middle row displays data from a second interrogator, where the signal response is somewhat degraded. The bottom row illustrates significant aliasing artifacts caused by an insufficient sampling rate in the third interrogator.

Specialized Tests

While the previously described tests characterize a system's fundamental response to various stimuli, certain operational scenarios in downhole environments present unique challenges that are not captured by static

benchmarks. Specifically, the rotation of the fiber at rotary joints during conveyance, the need to detect highly localized sub-meter events, and the effect of sensor motion relative to a stationary source all require specialized evaluation. This section details three tests designed to assess interrogator performance under these challenging, application-specific conditions. To facilitate these evaluations, a versatile test apparatus is constructed that integrates the necessary components for each scenario into a single testbed, as shown in Figure 10.

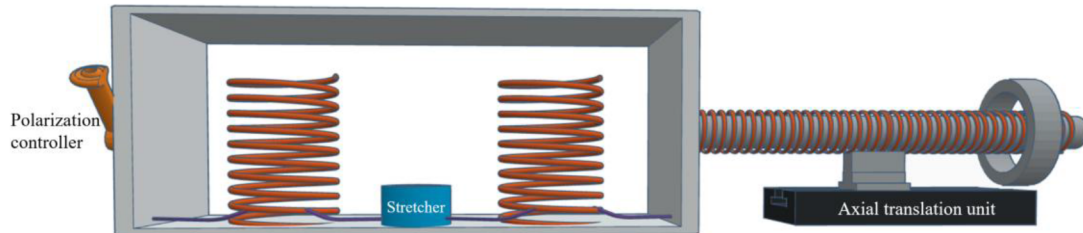


Figure 10—Specialized test apparatus that integrates the components for polarization sensitivity (polarization controllers), small-scale event detection (0.5 m piezoelectric stretcher), and dynamic thermal response (translation rig and stationary heat source).

Polarization Sensitivity Testing

In some downhole interventions, the fiber-optic cable is deployed via CT or wireline, which often requires a Fiber-Optic Rotary Joint (FORJ) to manage cable twist. While standard single-mode fiber does not preserve the state of polarization (SOP), a FORJ can exacerbate SOP instability by introducing rapid and unpredictable polarization changes during rotation. These fluctuations can induce additional variable signal loss and disrupt the interference of Rayleigh backscatter in phase-sensitive DAS systems, degrading phase demodulation accuracy and overall signal fidelity. To replicate this effect and test the interrogator's resilience to polarization variations, a series of polarization control devices are integrated into the fiber path (Figure 11). Three distinct mechanisms are used to manipulate the SOP: a three-paddle manual polarization controller, a programmable motorized polarization controller, and an actual FORJ unit identical to those used in field operations. Using these devices, the system is subjected to a series of controlled polarization scenarios. Specifically, near-fading, orthogonal, elliptical, and circular polarization states are induced and tested. For each of these scenarios, the primary performance metric evaluated is the system's self-noise, measured on a quiet section of fiber. This measurement quantifies the stability of the interrogator's output in the absence of an external acoustic signal, thereby isolating the noise induced purely by the changing SOP.



Figure 11—Devices used for polarization sensitivity testing. From left to right: a FORJ unit, a programmable motorized polarization controller, and a 3-paddle manual polarization controller. These devices are used to systematically alter the SOP of the light signal to test the interrogator's performance under dynamic polarization and loss conditions.

Small-Scale Mechanical Excitation

A critical application for DAS in flow monitoring is the detection of small-scale events, such as high-frequency acoustic signatures (small wavelengths), incipient leaks or sand production, which may only

excite a sub-meter section of the fiber. This capability is critical in advanced applications such as SoS tracking, as capturing higher wavenumbers significantly increases the confidence and accuracy of the resulting SoS measurement. While gauge length is a user-defined processing parameter, the system's true spatial resolution—its ability to distinguish highly localized events—is fundamentally constrained by hardware characteristics such as optical pulse width and receiver bandwidth, as well as by embedded signal processing routines specific to each interrogator. To measure this, a small-scale mechanical stimulus is applied using a piezoelectric fiber stretcher acting on a 0.5-meter segment of the fiber. This setup injects a precise mechanical waveform into a well-defined, localized region. The test is designed to assess two key performance metrics—namely, the minimum detectable event size and the effective spatial resolution of the DAS system under controlled conditions. The resulting DAS data is analyzed to determine the spatial spread of the measured signal. A high-resolution system shows the signal energy confined to a narrow zone corresponding to the 0.5-meter stretcher, whereas a lower-resolution system may exhibit spatial "smearing," where the event appears larger than its physical extent.

Figure 12 shows sample measured response to the excitation of the stretcher for two sample DAS systems, highlighting the difference in the spatial interval over which each system shows responsivity. The first system demonstrates a response that is well-localized to the physical extent of the stretcher, while the second system shows spatial smearing, indicating a lower effective resolution.

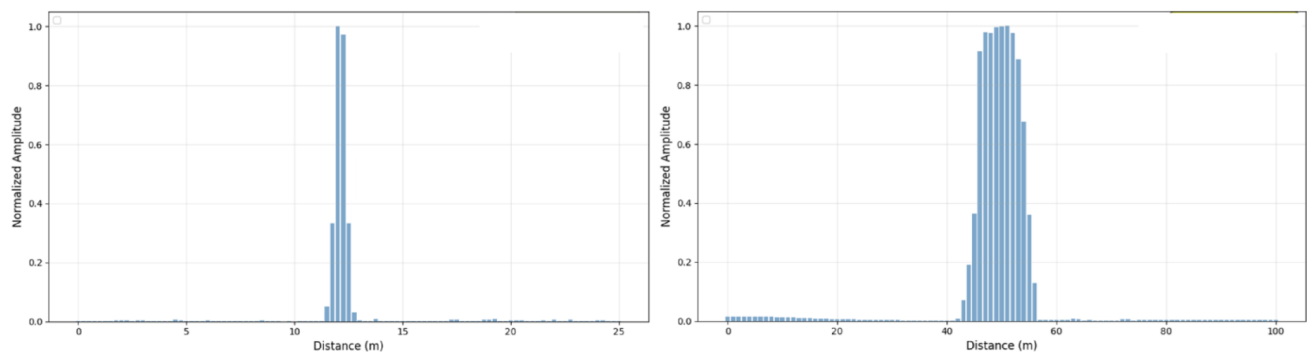


Figure 12—System response to small-scale mechanical excitation (0.5 m stretcher). Note the difference in the spatial extent (x-axis) of the measured signal, which demonstrates the noteworthy variation in true spatial resolution and localization capability between the two systems.

Plume Tracking and Dynamic Thermal Response Testing

In wireline or CT DAS monitoring projects, the fiber might be in continuous motion relative to the downhole environment. This introduces a dynamic component that is not present in static monitoring. To evaluate system performance under these conditions, a test is performed to measure the response to a thermal stimulus while the fiber is in motion. This setup also provides an opportunity to test the system's performance for low-frequency (LF) DAS applications, such as plume tracking. For this test, a portion of the fiber is mounted on a computer-controlled axial translation rig, which moves it at known constant velocities (e.g., 1 to 2 fpm). A stationary heat source provides a localized thermal stimulus. As the fiber moves past the heat source, the DAS system records the strain response, mimicking a logging tool moving past a thermal anomaly in a well, such as a leak or an injection/production zone. This test assesses the system's sensitivity to thermal disturbances (LF DAS) and its ability to accurately measure the thermal feature's amplitude and spatial extent without motion-induced distortion or smearing artifacts. This provides a direct measure of the system's fitness for dynamic logging applications.

Figure 13 shows sample LF DAS responses from three different interrogator systems, each using a 2-meter gauge length and data collected via a single-ended loopback fiber configuration. The logging was performed at three different velocities, increasing by approximately 25% from left to right. The second and third systems (middle and bottom plots) exhibit noticeable spatial smearing and heightened sensitivity

to changes in velocity, resulting in less clean datasets compared to the first system. Importantly, the same processing workflow was applied to the raw strain rate data across all systems, ensuring a direct and fair comparison of interrogator performance.

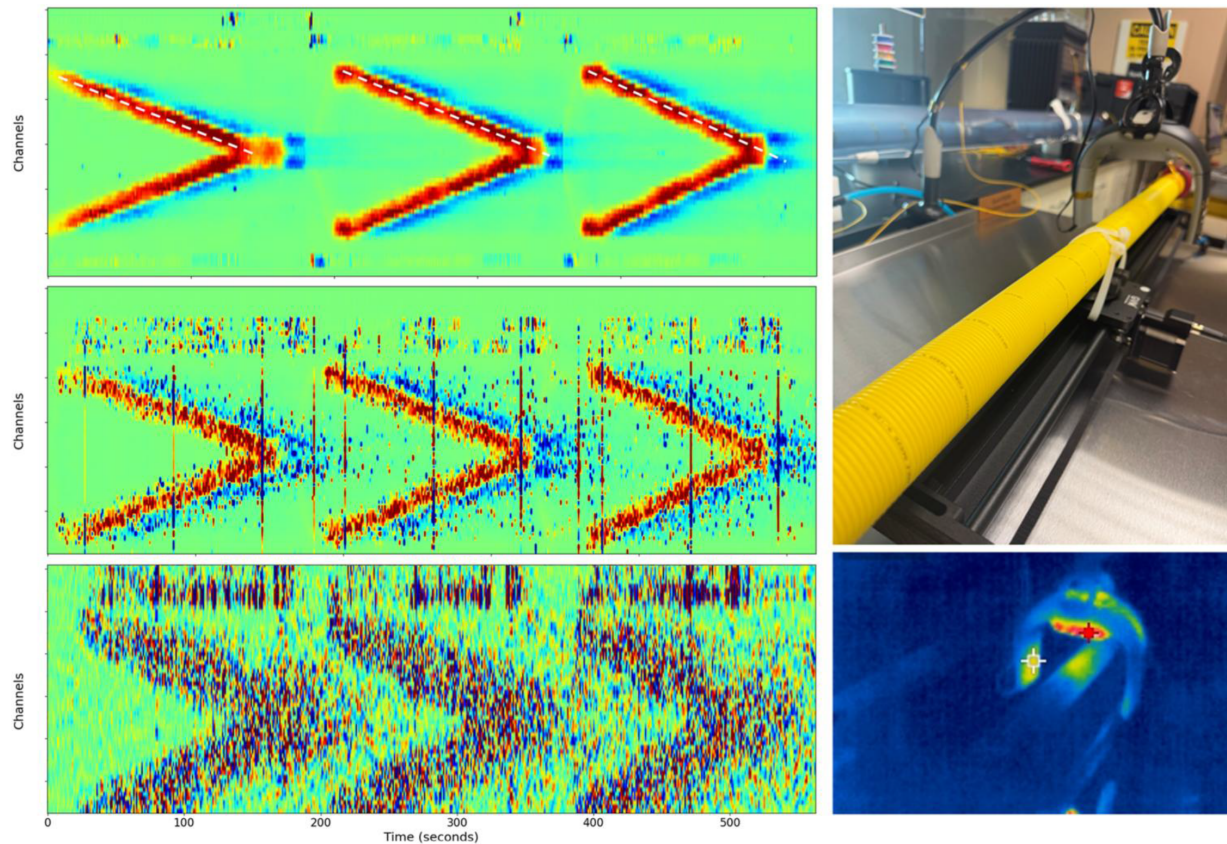


Figure 13—Comparison of dynamic thermal response for three DAS systems. The plots show LF DAS responses as a single-ended loopback fiber passes a stationary heat source at incrementally increasing velocities (left to right, ~25% per step). Recorded with a 2-meter gauge length, the second and third systems exhibit greater signal smearing and heightened sensitivity to velocity changes compared to the first system (top), which maintains cleaner response characteristics. These differences underscore varying suitability for dynamic logging applications.

Having evaluated the interrogators using a suite of novel, application-specific stimuli designed to mimic the unique challenges of downhole flow monitoring, we complete the evaluation with a series of fundamental performance tests. This final group utilizes a mechanical injection testbed designed in accordance with the principles outlined in the SEAFOM standard for DAS system qualification. Benchmarking against these established industry standards provides a complete performance profile, quantitatively measuring core metrics such as dynamic range, spatial resolution, and fidelity. These results complement the findings from the more specialized flow, acoustic, and dynamic tests, offering a comprehensive characterization of each interrogator's baseline capabilities.

Mechanical Waveform Injection

This group of tests utilizes a mechanical injection testbed designed in accordance with the principles outlined in the SEAFOM standard for DAS system qualification. The apparatus consists of 5 km of fiber, with three piezoelectric fiber stretchers positioned at distinct locations along its length, as depicted in Figure 14. This configuration mimics a 5 km wellbore with multiple points of stimulation. To better represent the small-scale events characteristic of flow monitoring, the stretchers used in this setup have a length of 8.5 meters. This testbed enables the quantitative measurement of key performance metrics including spatial

resolution, crosstalk, frequency response, dynamic range, and fidelity. Each test is designed to stimulate the fiber with controlled strain signals and assess interrogator’s response across various performance metrics. Signal generation and amplification equipment are used to precisely control amplitude and frequency of the injected waveforms.

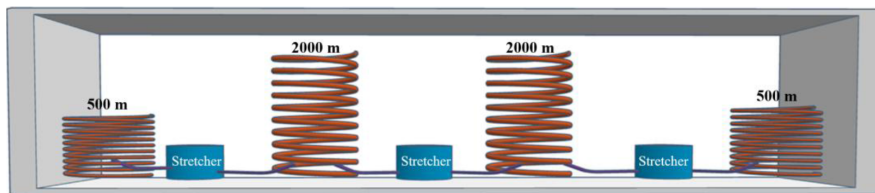


Figure 14—Mechanical waveform injection testbed designed based on SEAFOM recommended practices. The setup includes 5 km of fiber and multiple piezoelectric stretchers to simulate downhole acoustic events and perform quantitative performance testing.

Dynamic Range Test

The dynamic range test is performed to determine the maximum strain amplitude that the interrogator can accurately measure without introducing distortion. A sinusoidal signal is applied to each fiber stretcher at four discrete frequencies—1%, 5%, 20%, and 80% of the Nyquist frequency—while gradually increasing the amplitude from zero to a level beyond which the interrogator response becomes nonlinear. The strain amplitude is normalized by the gauge length to ensure consistency across different configurations. The onset of distortion, typically observed as phase discontinuities or waveform corruption, marks the upper limit of the dynamic range for each frequency and location. **Figure 15** plots sample dynamic range results for the four tested frequencies during the amplitude sweeps. The bottom two plots confirm a dynamic range of 124.1 dB; beyond this point, the system fails to maintain a linear response, and the output signal saturates.

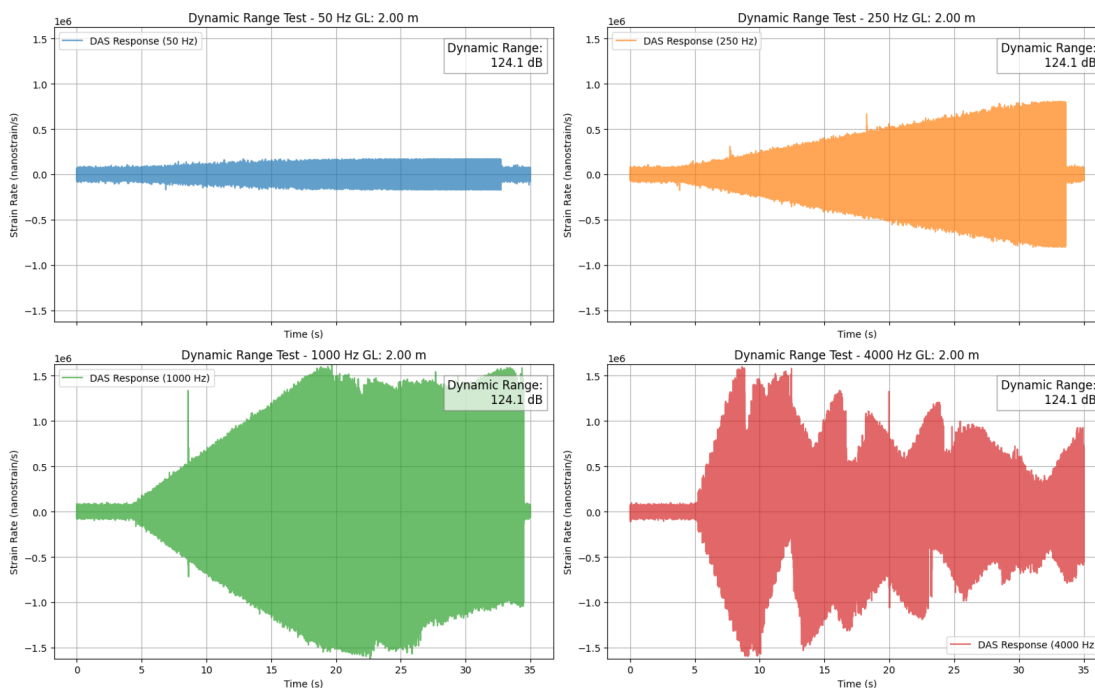


Figure 15—Dynamic range measurement at four different frequencies. The plots show the measured DAS output amplitudes. The system exhibits a linear response before reaching a saturation point. The dynamic range is determined by the difference between the noise floor and the onset of this non-linear behavior, confirmed here to be 124.1 dB.

Spatial Resolution Test

The spatial resolution test is designed to determine the minimum distance over which the interrogator can distinguish localized strain events. A sinusoidal signal at 2% of the Nyquist frequency is applied to a fiber stretcher, and data is collected from fiber sections spanning multiple gauge lengths on either side of the stimulus location. FFT analysis is used to extract the signal amplitude at each sensing location. The width of the transition region between high and low amplitude is then used to estimate the spatial resolution, which ideally should approximate the configured gauge length. Figure 16 illustrates the spatial response from two sample systems. The first system clearly shows a spatial resolution that matches the configured gauge length. In contrast, the plot on the right for the second system displays a broad peak spanning the location of the stretcher, demonstrating a lower effective spatial resolution and a reduced ability to localize the event.

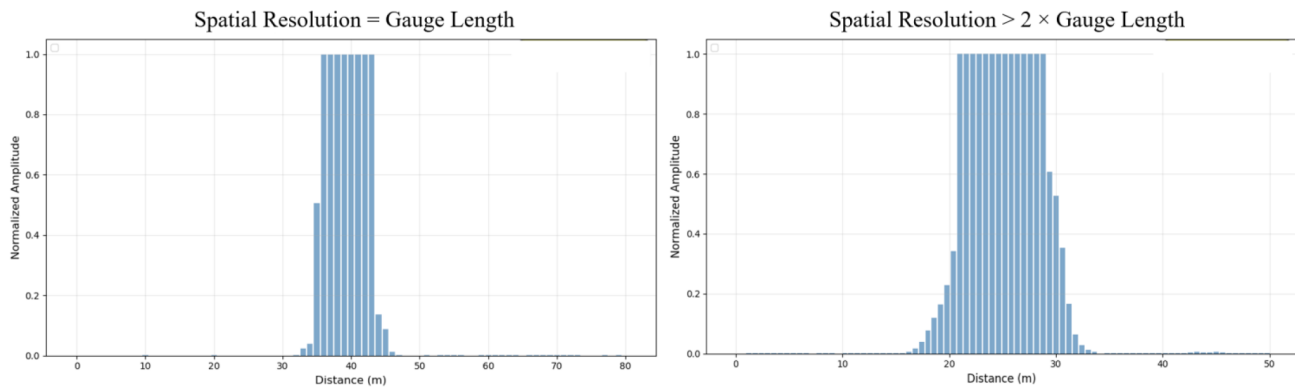


Figure 16—Comparison of spatial resolution for two DAS systems. The plot on the left shows a sharp response, with a spatial resolution that matches the configured gauge length. The plot on the right shows a smeared response with a broad peak, indicating a lower effective spatial resolution.

Crosstalk

To assess the presence of unintended signal leakage, crosstalk tests are performed using the same stimulus as in the spatial resolution test. Data is collected from fiber sections located multiple gauge lengths away from the active fiber stretcher. The signal amplitude at these remote locations is compared to the reference amplitude at the stimulus location, and the ratio is expressed in decibels. The resulting plots illustrate the extent of crosstalk and help identify any residual signals that could compromise measurement integrity. Figure 17 presents a comparative analysis of three sample DAS interrogators tested under identical interrogation parameters and stimulus conditions. System 1 demonstrates excellent signal isolation, maintaining a noise floor below -70 dB on adjacent channels. System 2 shows elevated noise levels on neighboring channels, indicating moderate crosstalk and reduced spatial confinement. System 3 exhibits pronounced downstream crosstalk beyond the excitation point, suggesting a higher risk of signal contamination.

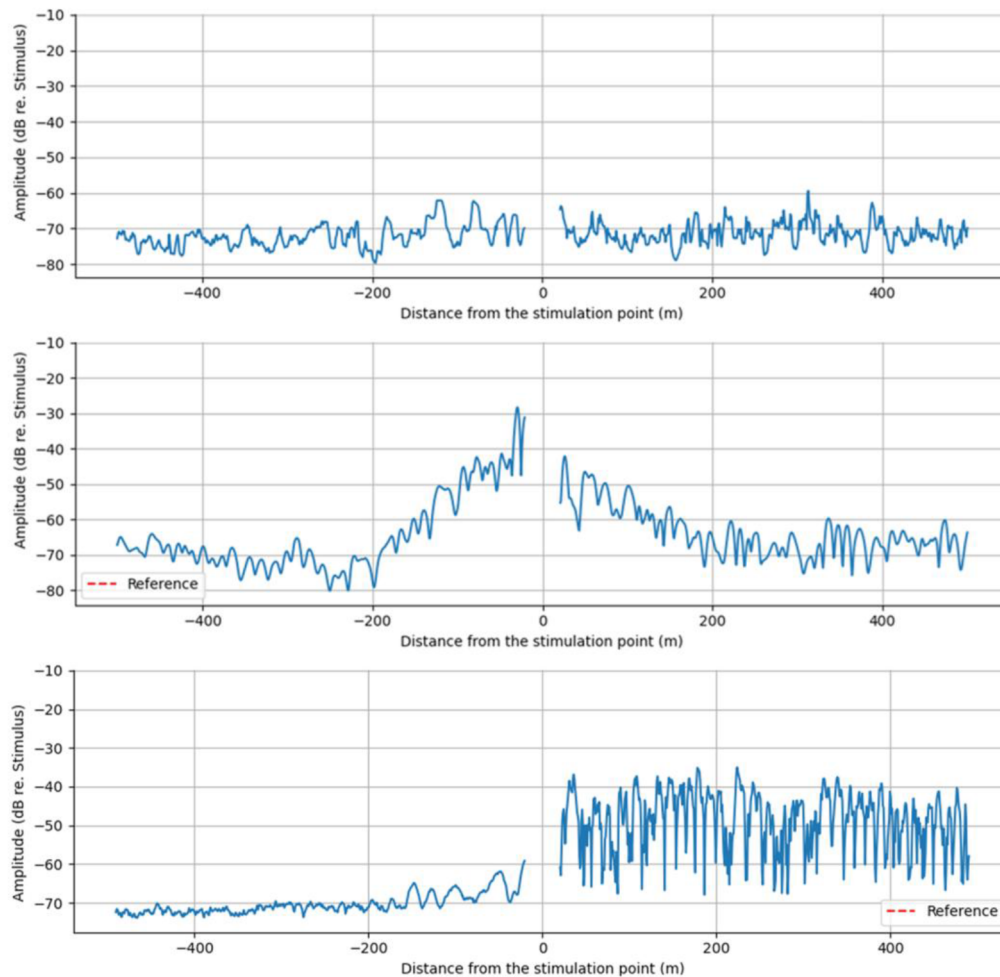


Figure 17—Crosstalk performance comparison for three DAS systems under identical mechanical excitation. The top plot (System 1) exhibits a low noise floor on channels adjacent to the excitation point ($\leq -60\text{ dB}$), indicating strong signal isolation. The middle plot (System 2) shows an elevated noise floor on neighboring channels, suggesting increased crosstalk. The bottom plot (System 3) reveals significant downstream crosstalk beyond the excitation point, indicating poor spatial confinement of the signal.

Frequency Response

To characterize the interrogator's sensitivity across its operational frequency range, frequency response tests are conducted using a stepped-frequency sinusoidal sweep. The stimulus consists of 40 discrete tones ranging from 2% to 80% of the Nyquist frequency. Each tone is applied for 2.5 seconds, resulting in a total sweep duration of 100 seconds, while the strain amplitude is held constant at 0.08 microstrain, normalized by the gauge length. The interrogator's output is transformed into the frequency domain using FFT analysis, and the magnitude of the response at each frequency is recorded. This process allows for the construction of both raw and normalized frequency response plots, revealing the interrogator's gain flatness and any frequency-dependent sensitivity variations. Figure 18 shows sample frequency response curves for two systems. The first system maintains a flat, consistent response across the entire tested frequency range, indicating uniform sensitivity. The second system's response begins to roll off, demonstrating a more limited effective bandwidth and non-uniform sensitivity across its operational range.

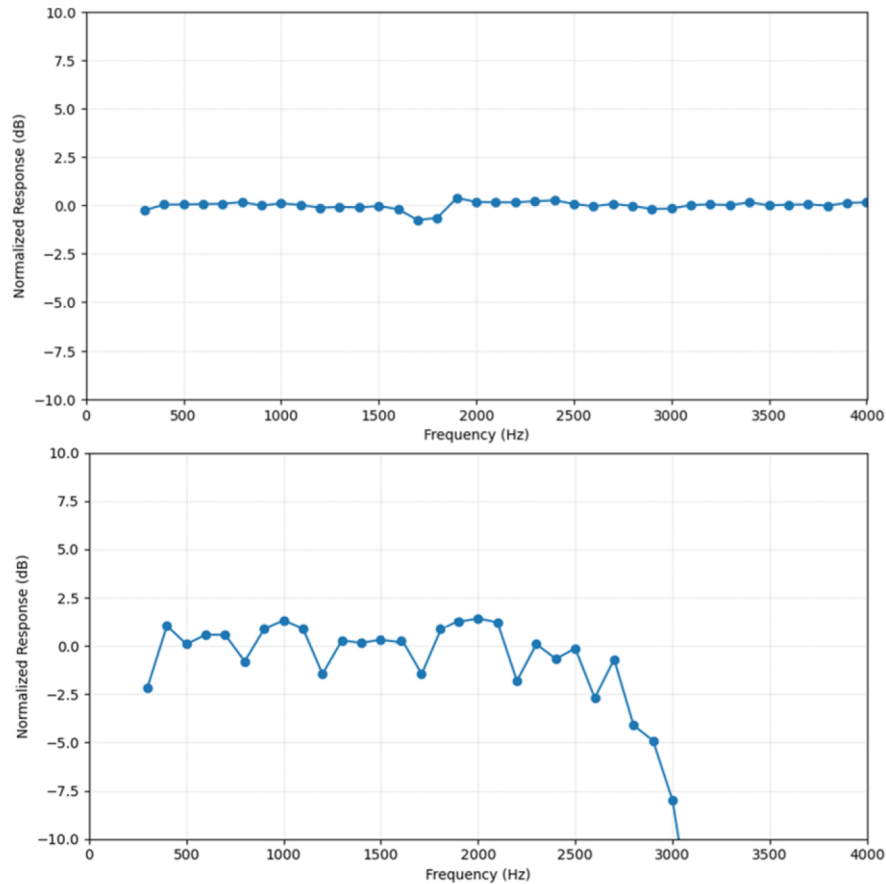


Figure 18—Frequency response comparison for two DAS systems. The top plot shows a flat response, indicating uniform sensitivity across the tested frequency range. The plot for the second system shows a noticeable roll-off, indicating a limited effective bandwidth.

Fidelity

The fidelity test assesses the interrogator's ability to reproduce a pure sinusoidal input signal without introducing harmonic distortion. A single-tone sinusoidal stimulus at 10% of the Nyquist frequency is applied at three amplitude levels: 0.08, 0.25, and 0.8 microstrain, normalized by the gauge length. The interrogator's output is segmented into time-series blocks and processed using a flat-top windowed FFT to isolate the fundamental frequency and its harmonics. Total Harmonic Distortion (THD) is calculated by comparing the power of the second through fifth harmonics to that of the fundamental. This metric provides a quantitative measure of the interrogator's signal purity and its susceptibility to nonlinear effects. [Figure 19](#) compares sample output spectrum from three systems when a pure sine wave is injected. The spectrum from the first system shows a single, sharp peak at the fundamental frequency with no visible harmonics. The spectrum from the last two systems shows significant harmonic peaks at multiples of the fundamental frequency, indicating high THD and poor fidelity. The third system not only shows elevated harmonic content but also suffers from aliasing artifacts—some harmonics fold back into the baseband due to an insufficient sampling rate, further degrading spectral clarity and confounding the interpretation of true signal content.

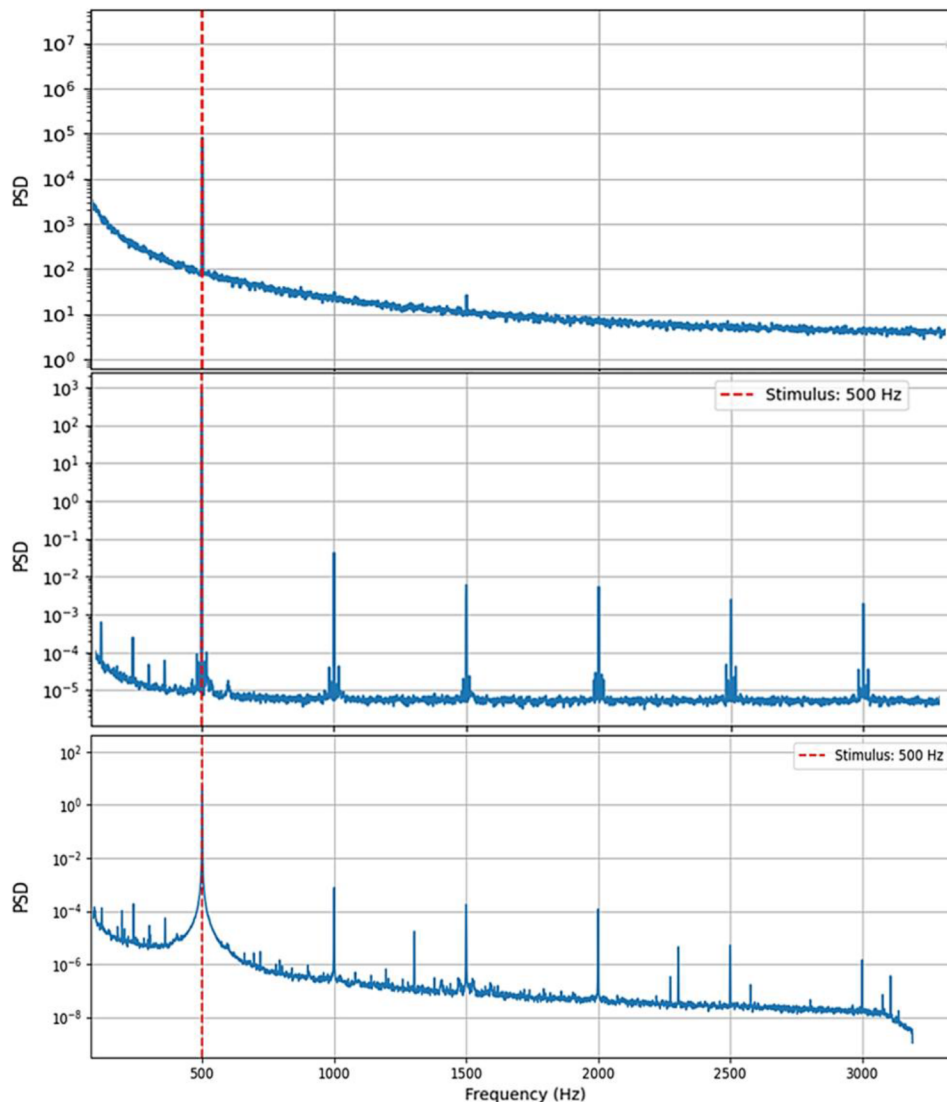


Figure 19—Sample fidelity test results. The output spectrum for the first system shows a clean, single peak at the fundamental frequency, indicating low THD. The spectrum for the second and third systems shows significant harmonic peaks, indicating high THD and lower fidelity.

Summary

We presented systematic workflow for benchmarking the performance of DAS interrogators, with a specific focus on the demanding requirements of downhole flow monitoring applications. By subjecting various interrogators to a suite of controlled and realistic stimuli—including turbulent flow, complex acoustic waveforms, dynamic polarization changes, and localized mechanical and thermal events—and by utilizing both standard and engineered fiber, we moved beyond conventional testing standards to provide a more holistic and application-relevant assessment of system capabilities (Figure 20–21). The findings underscore that DAS system and fiber selection must be guided by rigorous, application-specific testing. A "one-size-fits-all" approach is insufficient, for instance, an interrogator optimized for low-frequency seismic applications may not possess the broadband fidelity, phase stability, or dynamic range required for quantitative flow monitoring. Therefore, it is strongly recommended that operators and service providers adopt a tailored benchmarking methodology to certify that a system is fit-for-purpose before a critical field deployment. Moreover, given that DAS interrogators are complex optoelectronic instruments, their performance can drift or degrade over time. A factory acceptance test is a necessary but not sufficient condition for ensuring long-term data quality. We recommend that the performance of these systems be re-

evaluated periodically or before major projects to mitigate operational risk and ensure that the collected data remains reliable and quantitative. By establishing and adhering to such robust testing standards, the industry can more effectively harness the full potential of DAS technology, moving from qualitative observation to quantitative characterization of downhole flow dynamics.

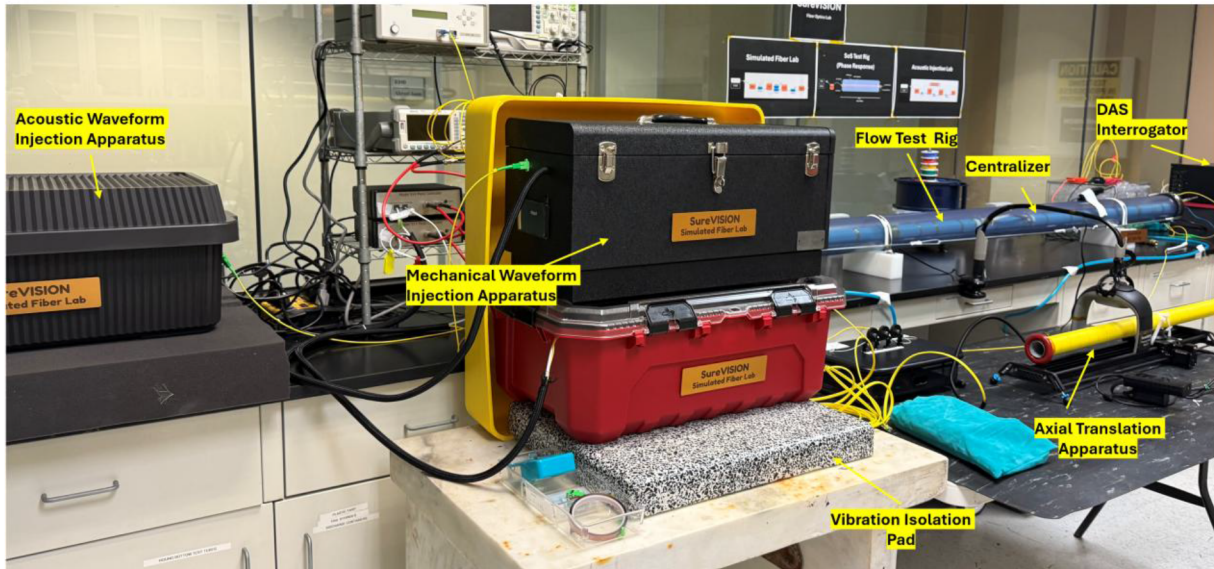


Figure 20—Simulated fiber optics laboratory facility for DAS interrogator benchmarking. Key apparatus shown includes the turbulent flow loop, the acoustic test box, and the mechanical injection testbed with fiber spools. This integrated setup enables the comprehensive suite of mechanical, acoustic, and flow-based stimuli detailed in this study.

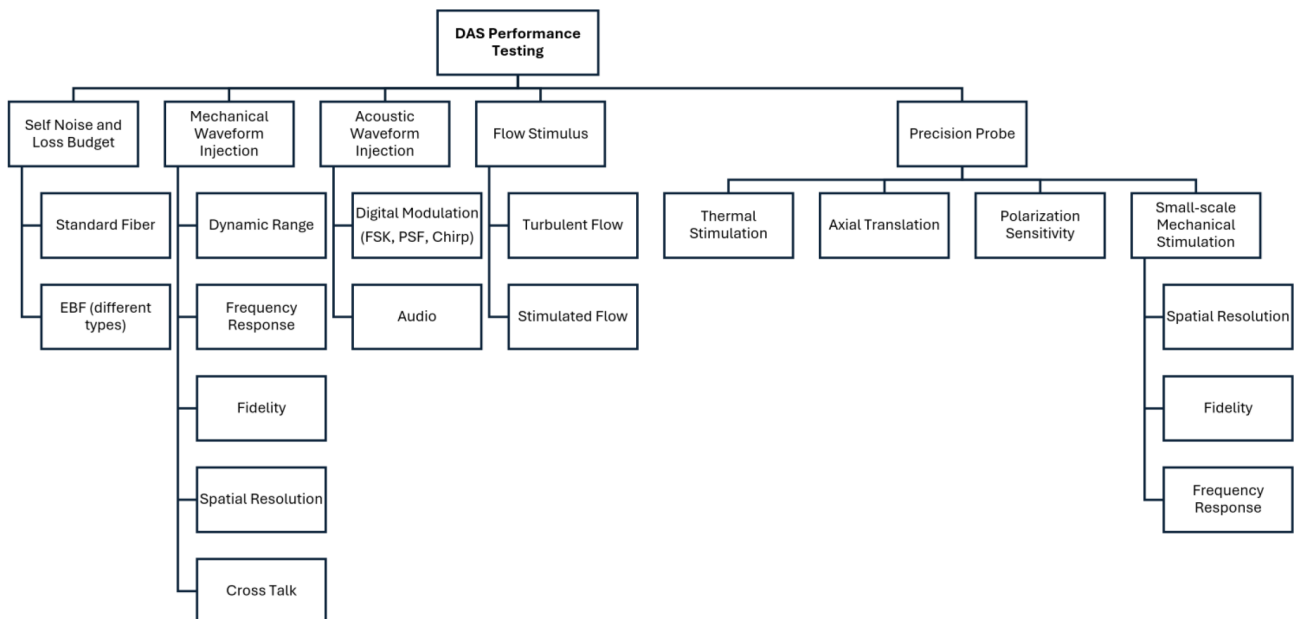


Figure 21—Full suite of experimental methodologies used to evaluate DAS system performance. Tests span five major categories: (1) Self Noise and Loss Budget; (2) Mechanical Waveform Injection; (3) Acoustic Waveform Injection; (4) Flow Stimulus; and (5) Precision Probe—involving axial translation, polarization sensitivity, and small-scale mechanical stimulation with resolution and fidelity metrics.

References

1. Daley, T. M., Freifeld, B. M., Ajo-Franklin, J., Dou, S., Pevzner, R., Shulakova, V., Lueth, S. (2013). Field testing of fiber-optic distributed acoustic sensing (DAS) for subsurface seismic monitoring. *The Leading Edge*, **32**(6), 699–706.
2. Farhadiroushan, M., Milne, C., Parker, T., Hafezi, S., Aghayev, R., Mahue, V., Shatalin, S. (2021, March). Engineered Distributed Acoustic Flow Profiling Sensing Solutions. *EAGE GeoTech 2021 Second EAGE Workshop on Distributed Fibre Optic Sensing* (Vol. **2021**, No. 1, pp. 1–5).
3. Hull, R. A., Meek, R., Bello, H., Miller, D. (2017). *Case history of DAS fiber-based microseismic and strain data, monitoring horizontal hydraulic stimulations using various tools to highlight physical deformation processes (Part A)*. Unconventional Resources Technology Conference (pp. 3050–3062).
4. Lindsey, N. J., Rademacher, H., Ajo-Franklin, J.B. (2020). On the broadband instrument response of fiber-optic DAS arrays. *Journal of Geophysical Research: Solid Earth*, **125**(2), e2019JB018145.
5. Subsea Fiber Optic Monitoring (SEAFOM) Group. (n.d.). *Measuring Sensor Performance – DAS Parameter Definitions and Tests*. Retrieved, from <https://seafom.com/published-documents>
6. Moradi, P. (2025). *SoundBal: Two-Phase Production Logging by Integrating Mass Balance and DAS-Based Speed of Sound*. SPE/AAPG/SEG Unconventional Resources Technology Conference (p. D031S063R001).
7. Moradi, P., Seabrook, B., Adair, N., Garza, R. (2024). *Resolving multiphase fractions in horizontal wells using speed of sound measured with distributed acoustic sensors and a PVT database*. SPE/AAPG/SEG Unconventional Resources Technology Conference (p. D021S031R001).
8. Ünal, Ö. H. (2022). *Downhole three-phase flow measurement using sound speed measured by local or distributed acoustic sensing*. SPE Annual Technical Conference and Exhibition (p. D021S032R002). SPE.
9. Verdon, J. P., Horne, S. A., Clarke, A., Stork, A. L., Baird, A. F., Kendall, J. M. (2020). Microseismic monitoring using a fiber-optic distributed acoustic sensor array. *Geophysics*, **85**(3), KS89–KS99.
10. Xiao, J., Farhadiroushan, M., Clarke, A., Jacob, S., AlMulhem, A., Milne, H. C., Parker, T. (2015). *Dynamic water injection profiling in intelligent wells using distributed acoustic sensor with multimode optical fibers*. SPE Annual Technical Conference and Exhibition (p. D021S020R004).